RTSA
GLOBAL PERSPECTIVES
CORE2012
CONFERENCE ON RAILWAY ENGINEERING
10-12 SEPTEMBER 2012 BRISBANE AUSTRALIA

COMPARATIVE ASSESSMENT OF INSULATED RAIL JOINT ASSEMBLIES

Peter Mutton[1], Cameron Thompson[1], Mina Hanna[1], Stephen Oswald [2] and Leon Wessels[2]

[1] **Institute of Railway Technology, Monash University**

[2] **Rio Tinto Iron Ore**

SUMMARY

Insulated rail joint (IRJ) assemblies are subjected to increased dynamic loading relative to adjacent track, often in conjunction with poor track support conditions, such that their service performance is compromised. This situation is exacerbated under high axle load, heavy haul conditions, often resulting in premature failure. A metallurgical failure analysis has confirmed that fatigue failure of joint bars in the IRJ type currently used is associated with the presence of near-surface decarburisation, which results in a significant reduction in fatigue strength relative to the core material. The currently-used IRJ design and three alternative designs have been subjected to a laboratory test program which included measurement of joint bar strains under a range of loading conditions, fatigue testing under conditions which have been found to reproduce the in-service failure mode, and the properties of the joint bar materials. The results have been used to rank the four designs in terms of the probability of joint bar fatigue failures. The test program provides a basis for specifying qualification requirements for insulated rail joints to be used under heavy haul conditions.

INTRODUCTION

Insulated rail joint (IRJ) assemblies, in combination with track circuitry, fulfil a safety-critical function in the form of broken rail detection. However IRJ assemblies may be subjected to increased dynamic loading relative to adjacent track, often in conjunction with poor track support conditions, such that their service performance is compromised. This situation is exacerbated under the high axle load, heavy haul conditions typical of mining railways, often resulting in premature failure.

The relatively poor service performance of IRJ assemblies in other sectors of the railway industry has prompted a number of initiatives aimed at improving their reliability [1-6]. These include reconfiguring the end post, alternative joint bar designs, bonding systems, and improving the track support conditions.

The work described in this paper formed part of a program undertaken to improve the service performance of IRJ assemblies under heavy haul conditions. The IRJ type used under these conditions has been found to fail prematurely as a result of fatigue cracking which develops in the joint bars.

The primary emphasis in the work described was the structural behaviour of the IRJ assemblies, with particular emphasis on the failure mode commonly observed in service. The program covered:

(a) metallurgical failure analysis on joint bars from two failed IRJs, in order to identify any material-related factors that contributed to the failures;

(b) assessment of the currently-used IRJ design, and several alternative glued IRJ designs, in terms of the response under static and cyclic loading conditions and the characteristics of the joint bar materials.

The results of the test program are discussed in the context of qualification requirements for both IRJ assemblies and joint bar materials, in order to develop more rigorous acceptance requirements for heavy haul conditions.

In addition to the laboratory test program described in the current paper, joint bars stress levels measured under the relevant service loading conditions are discussed in a separate (unrelated) paper [7].

EXAMINATION OF FAILED JOINT BARS

Three failed joint bars from IRJ assemblies that had been in service at two different track locations were supplied for examination. The failure mode in each joint bar was identical, and resulted from fatigue cracking which initiated at the lower outer corner of the joint bar (Figure 1). The joint bars then fractured in a brittle mode when the fatigue cracks had propagated to a maximum crack length of 17-19mm.

Cover
Foreword
Concurrent Session 1: ROLLING STOCK COMPONENTS
Concurrent Session 2: RAIL
Concurrent Session 3: RAIL SAFETY
Concurrent Session 4: RAIL CAPACITY
Concurrent Session 5: WHEEL/RAIL
Concurrent Session 6: CIVIL STRUCTURES
Concurrent Session 7: SAFETY MANAGEMENT & SIGNALLING
Concurrent Session 8:
Concurrent Session 9: ROLLING STOCK MODELLING
Concurrent Session 10: TRACK STRUCTURE
Concurrent Session 11: CIVIL STRUCTURES
Concurrent Session 12: ELECTRICAL O/H
Concurrent Session 13: WHEEL/RAIL
Concurrent Session 14: PROJECT MANAGEMENT
Concurrent Session 15: ENERGY
Concurrent Session 16: INNOVATION
Concurrent Session 17: ROLLING STOCK
Concurrent Session 18: TRACK CONDITION MONITORING
Concurrent Session 19: ELECTRICAL OVERHEAD
Author Index
Close Document

or were specifically manufactured for the study using different joint bar materials, were subjected to a test program which covered the following aspects:

(a) load-deflection and load-joint bar strain behaviour under static loading;

(b) fatigue behaviour when tested in accordance with the relevant Australian standard [11], and under more severe loading conditions which were expected to reproduce the in-service failure mode in the currently-used design; and

(c) mechanical properties of the joint bar materials.

Details of the four IRJ assemblies are summarised in Table 1. Figure 5 shows the cross-section of Types A, B and D IRJ assemblies; Type C was identical in appearance to Type A.

The Type B design incorporates a forged joint bar in which the lower flange is wider over the central region; Figure 5 shows the cross-section at the mid-point of the joint bar. In all three other types the joint bars were uniform in cross section over the entire length.

The joint bars in Types C and D were manufactured specifically for the test program; those in Types A and B are commercially available. All IRJ's were assembled using a 68kg/m, hypereutectoid heat treated rail grade identical to that used in service.

Measurement of joint bar strains and load-deflection behaviour

One IRJ assembly of each type was instrumented with strain gauges for the measurement of longitudinal strains at the mid-point of the upper and lower flanges, as shown in Figure 6. This position was identical to that used previously for the in-track instrumentation [7].

Measurement of the load/deflection behaviour and corresponding joint bar strains was carried out with each of the instrumented IRJ assemblies simply supported on 3-point loading as required by AS1085.12 for the load deflection test [11]. Figure 7 shows the general loading arrangement.

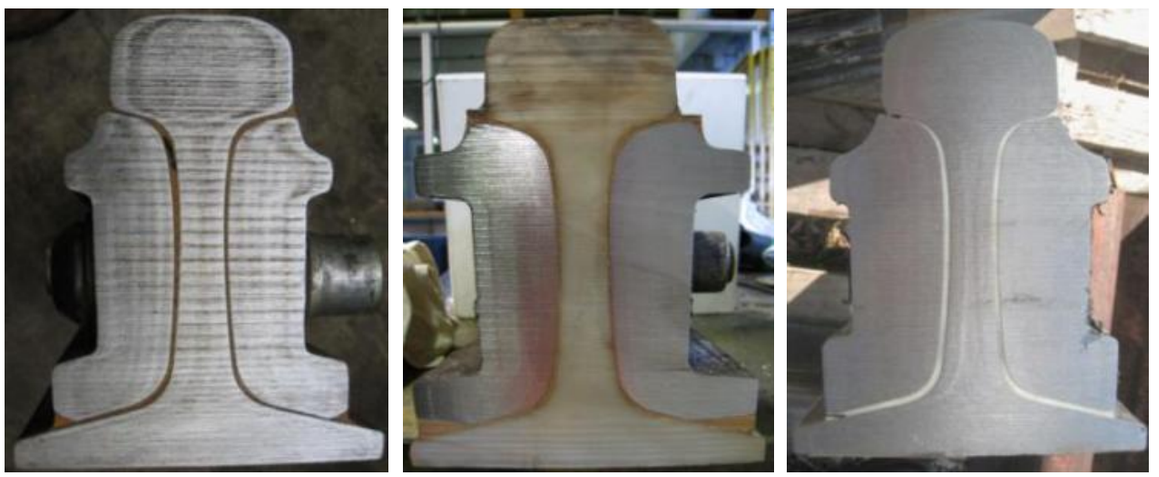
One set of measurements were taken with each IRJ type loaded to a maximum of 1350kN, as specified in AS1085.12 for IRJ assemblies in 68kg rail [11]. The measurements were then repeated to a maximum load of 2000kN.

Table 2 summarises the results of the load-deflection tests in terms of the maximum deflection at the specified test load of 1350kN, the residual deflection, and the maximum deflection at the higher test load (2000kN). The Type C design did not reach the maximum load in the second test, due to breakdown in the adhesive bonding.

The load versus joint bars strain behaviour of all four IRJ designs is summarised in Figure 8 (a) and 8(b), for the 1350kN and 2000kN tests respectively.

Table 1: Summary of IRJ assemblies

Type	*Joint bar manufacture*	*Assembly method*	*Comments*
A	Hot rolled section	Glued and Huck-bolted	Microalloyed steel; type currently used
B	Forged	Glued and Huck-bolted	Heavier, non-uniform joint bar section
C	Machined	Glued and Huck-bolted	Copy of Type A design, with alternative joint bar material (Hot rolled QT steel)
D	Machined	Glued and bolted	Heavier joint bar section than Types A and C



Type A ***Type B (mid-point of joint bar)*** ***Type D***

Figure 5 : Joint bar details in IRJ assemblies

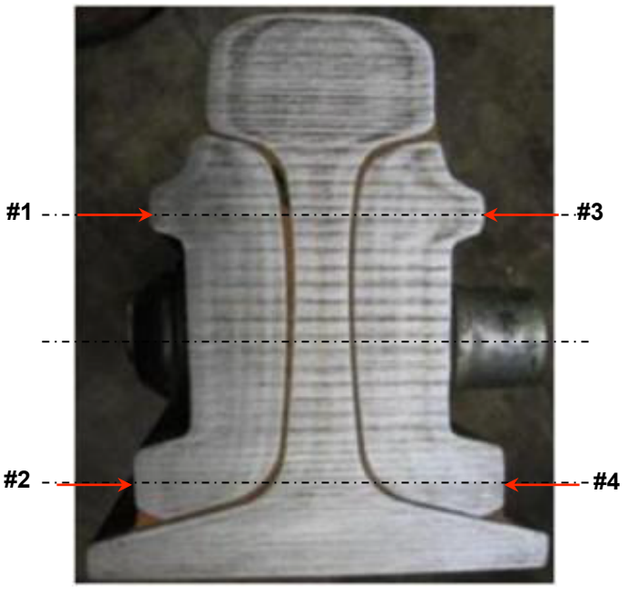


Figure 6 : Location of strain gauges (all IRJ types)

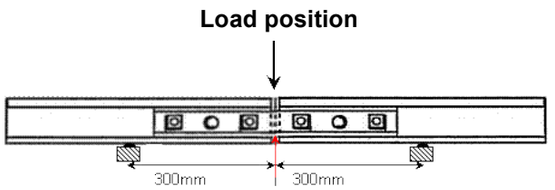
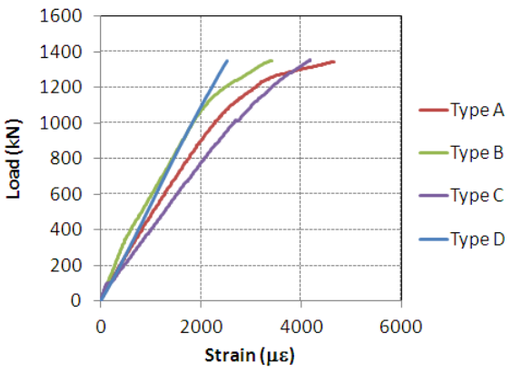


Figure 7 : Loading arrangement for load-deflection tests [11]

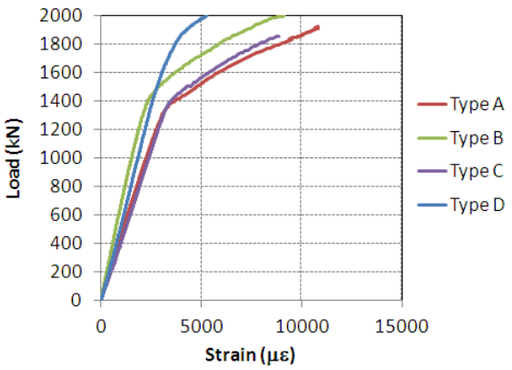
Table 2: Load-deflection test results

Type	*Test load (kN)*	*Maximum deflection (mm)*	*Residual deflection (mm)*
A	1350	2.73	0.30
	2000	6.21	2.47
B	1350	3.91	1.91
	2000	7.57	3.65
C	1350	3.47	0.25
	1859	5.70	(Failed)
D	1350	2.33	0.26
	2000	3.43	0.29

For the 1350kN test, the four designs differed slightly in their response in the elastic range, as expected from the differences in joint bar design. Types A, B and C exhibited plastic behaviour at loads above 1000kN; the extent of plastic strain was less with the higher strength joint bar material in Type C, and the highest with the Type A design with the hot rolled microalloyed joint bars. The Type D design exhibited negligible plastic strain up to the maximum load of 1350kN.



(A) 1350kN load



(B) 2000kN load

Figure 8 : Load/joint bar strain behaviour, lower gauge positions,

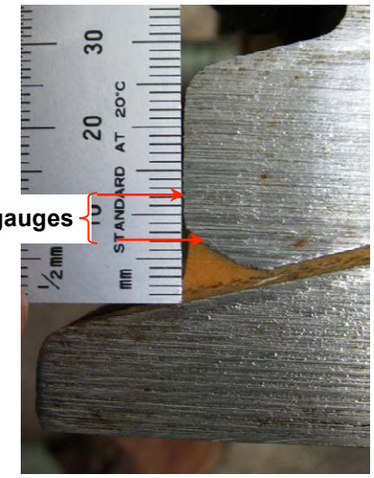
In the 2000kN test, Types A, B and C exhibited elastic behaviour up to the previous test load (1350kN), and thereafter increased plastic deformation, while the Type D design only exhibited plastic behaviour at loads above 1700kN.

Fatigue testing

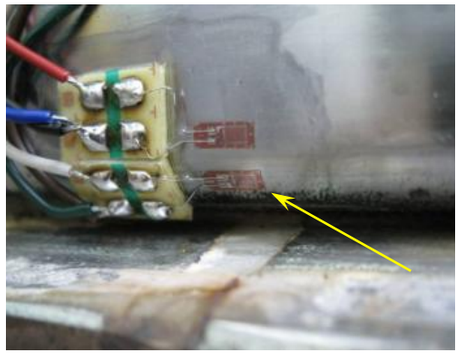
Two assemblies of each of design were subjected to fatigue testing in accordance with the requirements of AS1085.12 Appendix F [11], i.e. 3-point loading at a support span of 1100mm, a load range of 10-290kN, and test duration of 3 million cycles. At the completion of each test, a second test was carried out on each assembly at a load range of 10-400kN for a test duration of 3 million cycles..

The joint bar stress data obtained from the static measurements was used to estimate the equivalent stress levels under the fatigue test conditions. For the Type A design only, additional strain gauges were installed at slightly lower positions on the lower flange of the joint bars in a further IRJ assembly, in order to examine in more detail the stress distribution in the region subjected to fatigue cracking. Figure 9 shows the position of the two additional gauges; the lower position corresponded to the position of fatigue crack initiation in the joint bars which had failed in service.

Cover
Foreword
Concurrent Session 1: ROLLING STOCK COMPONENTS
Concurrent Session 2: RAIL
Concurrent Session 3: RAIL SAFETY
Concurrent Session 4: RAIL CAPACITY
Concurrent Session 5: WHEEL/RAIL
Concurrent Session 6: CIVIL STRUCTURES
Concurrent Session 7: SAFETY MANAGEMENT & SIGNALLING
Concurrent Session 8:
Concurrent Session 9: ROLLING STOCK MODELLING
Concurrent Session 10: TRACK STRUCTURE
Concurrent Session 11: CIVIL STRUCTURES
Concurrent Session 12: ELECTRICAL O/H
Concurrent Session 13: WHEEL/RAIL
Concurrent Session 14: PROJECT MANAGEMENT
Concurrent Session 15: ENERGY
Concurrent Session 16: INNOVATION
Concurrent Session 17: ROLLING STOCK
Concurrent Session 18: TRACK CONDITION MONITORING
Concurrent Session 19: ELECTRICAL OVERHEAD
Author Index
Close Document
Search



(A) Cross section at centreline



(B) Strain gauges

Figure 9 : Positions of additional strain gauges (Type A only). Lower position (arrowed) corresponds to position of fatigue crack initiation

The stress data are plotted as a function of the strain gauge position in Figures 10 and 11. At the lower gauge locations, the currently-used IRJ design (with both hot rolled (Type A) and machined (Type C) joint bars) exhibited the highest stress levels, and the Type B and D designs the lowest.

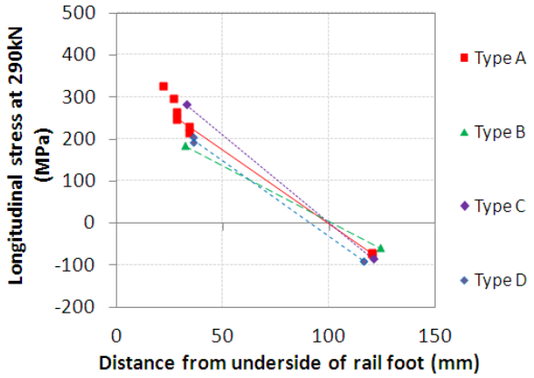


Figure 10: Joint bar stress levels under 290kN load fatigue test conditions

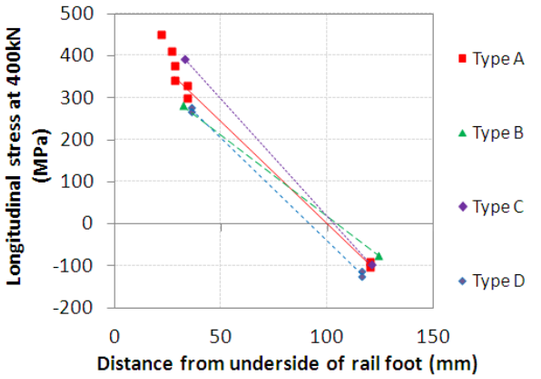


Figure 11: Joint bar stress levels under 400kN load fatigue test conditions

Figure 12 summarises the deflection measured under the maximum load, prior to commencement of each fatigue test; the values shown are the average for the two assemblies of each type tested. All four types gave similar deflections at the lower test load; however at the higher test load the Type A design exhibited significantly higher mean deflection than the other types.

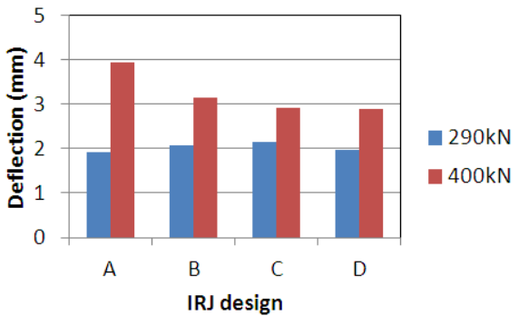


Figure 12 : Mean deflection measurements under fatigue test conditions

Failure of one of the Type A IRJ assemblies occurred after 1.3 million cycles at the higher test load of 400kN. The failure mode was identical to that identified in the in-service failures, i.e. due to a fatigue crack which initiated in one joint bar at the identical position to the in-service failures, as shown in Figure 13. All other IRJ assemblies completed 3 million cycles at both load ranges without failure.

Assessment of joint bar materials

One joint bar from each IRJ type was sectioned for determination of the material characteristics, using the same procedure as outlined above for the joint bars which failed in service. The results of these tests are summarised in Table 3.

Figure 14 shows the near-surface hardness distribution at the lower corner of the joint bars. Figure 15 shows near-surface microstructures in the Type B, C and D joint bars; the corresponding microstructure in the Type A joint bars was identical to that shown in Figure 2.

Cover
Foreword
Concurrent Session 1: ROLLING STOCK COMPONENTS
Concurrent Session 2: RAIL
Concurrent Session 3: RAIL SAFETY
Concurrent Session 4: RAIL CAPACITY
Concurrent Session 5: WHEEL/RAIL
Concurrent Session 6: CIVIL STRUCTURES
Concurrent Session 7: SAFETY MANAGEMENT & SIGNALLING
Concurrent Session 8:
Concurrent Session 9: ROLLING STOCK MODELLING
Concurrent Session 10: TRACK STRUCTURE
Concurrent Session 11: CIVIL STRUCTURES
Concurrent Session 12: ELECTRICAL O/H
Concurrent Session 13: WHEEL/RAIL
Concurrent Session 14: PROJECT MANAGEMENT
Concurrent Session 15: ENERGY
Concurrent Session 16: INNOVATION
Concurrent Session 17: ROLLING STOCK
Concurrent Session 18: TRACK CONDITION MONITORING
Concurrent Session 19: ELECTRICAL OVERHEAD
Author Index
Close Document
Search



Figure 13 : Fatigue crack in joint bar of Type A design, 400kN test

The Type A joint bar exhibited similar levels of decarburisation to those which failed in service, whereas the extent of decarburisation in the Type B (High Modulus) joint bar was slightly greater. No decarburisation was evident in the two machined joint bars (Types C and D).

All joint bar materials complied with the AREMA tensile requirements.

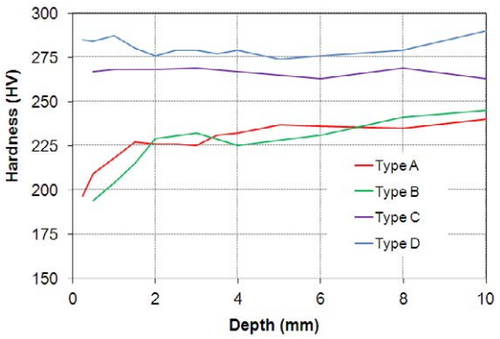
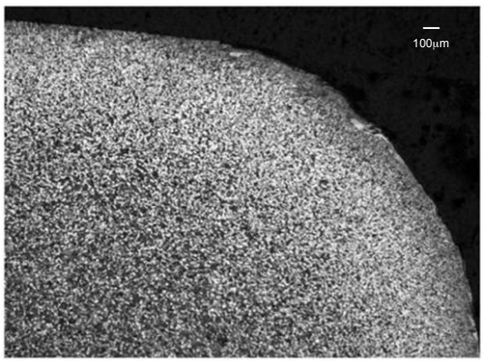
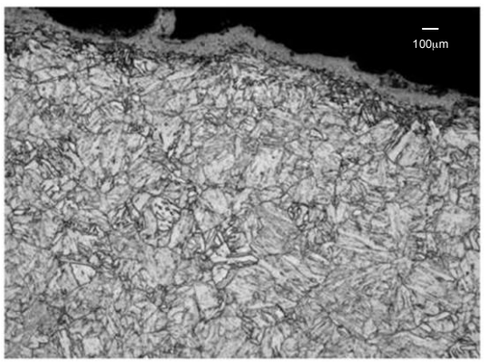


Figure 14 : Near-surface hardness distribution in joint bars



(A) Type B



(B) Type C



(C) Type D

Figure 15 : Near-surface microstructure in joint bars

Table 3: Joint bar material properties

Type	*0.2% Proof stress (MPa)*	*Tensile strength (MPa)*	*El. (%)*	*RoA (%)*	*Depth of decarb. (mm)*	*Core hardness (HV10)*	*Microstructure*
A	565	798	22	62	1.5	242	Ferrite/pearlite
B	514	778	21	59	2	250	Spheroidised pearlite/bainite
C	650	735	19	69	Nil	267	Tempered martensite
D	699	894	13	47	Nil	284	Tempered martensite
AREMA	483 min	689 min	12 min	25 min	1.02 max	Not specified	Not specified

Cover
Foreword
Concurrent Session 1: ROLLING STOCK COMPONENTS
Concurrent Session 2: RAIL
Concurrent Session 3: RAIL SAFETY
Concurrent Session 4: RAIL CAPACITY
Concurrent Session 5: WHEEL/RAIL
Concurrent Session 6: CIVIL STRUCTURES
Concurrent Session 7: SAFETY MANAGEMENT & SIGNALLING
Concurrent Session 8:
Concurrent Session 9: ROLLING STOCK MODELLING
Concurrent Session 10: TRACK STRUCTURE
Concurrent Session 11: CIVIL STRUCTURES
Concurrent Session 12: ELECTRICAL O/H
Concurrent Session 13: WHEEL/RAIL
Concurrent Session 14: PROJECT MANAGEMENT
Concurrent Session 15: ENERGY
Concurrent Session 16: INNOVATION
Concurrent Session 17: ROLLING STOCK
Concurrent Session 18: TRACK CONDITION MONITORING
Concurrent Session 19: ELECTRICAL OVERHEAD
Author Index
Close Document
Search

Cover
Foreword
Concurrent Session 1: ROLLING STOCK COMPONENTS
Concurrent Session 2: RAIL
Concurrent Session 3: RAIL SAFETY
Concurrent Session 4: RAIL CAPACITY
Concurrent Session 5: WHEEL/RAIL
Concurrent Session 6: CIVIL STRUCTURES
Concurrent Session 7: SAFETY MANAGEMENT & SIGNALLING
Concurrent Session 8:
Concurrent Session 9: ROLLING STOCK MODELLING
Concurrent Session 10: TRACK STRUCTURE
Concurrent Session 11: CIVIL STRUCTURES
Concurrent Session 12: ELECTRICAL O/H
Concurrent Session 13: WHEEL/RAIL
Concurrent Session 14: PROJECT MANAGEMENT
Concurrent Session 15: ENERGY
Concurrent Session 16: INNOVATION
Concurrent Session 17: ROLLING STOCK
Concurrent Session 18: TRACK CONDITION MONITORING
Concurrent Session 19: ELECTRICAL OVERHEAD
Author Index
Close Document

DISCUSSION

Examination of the joint bars which failed in service, and the results of the laboratory tests in the currently-used IRJ type and 3 alternative types, indicate that while they may all comply with the relevant specifications, they differ in terms of both the joint bar characteristics and their behaviour under cyclic loading conditions. The test results can therefore be used to rank the four types in terms of their expected service performance under heavy haul conditions, which was the primary objective of the laboratory test program.

The four IRJ designs varied in terms of:

- The dimensions of the joint bars, with the Type D design having the largest overall uniform cross section, and the Type A design the smallest;
- The strength of the joint bar material, as measured during tensile testing; and
- The extent of near-surface decarburisation, particularly in the critical region at the bottom surface.

The Type D design was ranked the best overall, with a combination of heavier joint bars of higher strength material and an absence of near-surface decarburisation. The Type C design with the machined QT steel joint bars ranked better than the Type A design with the hot rolled micro-alloyed joint bars, due to the absence of near-surface decarburisation in the former. The Type B design provided some advantages over the standard design due to the heavier joint bar section dimensions; however these joint bars exhibited the greatest near-surface decarburisation and the lowest yield strength of any of the joint bar materials examined.

The test results can also be used to examine the qualification requirements for insulated rail joint assemblies, particularly those to be used under heavy haul conditions. For Australian rail systems these are described in the relevant Australian [11] standard. However for IRJ assemblies used in heavy haul systems in the Pilbara, some components may be manufactured in North America, and hence may be manufactured to comply with the corresponding AREMA requirements [8]. In addition, joint bars or fishplates may be qualified according to either AS1085.2 [12], or the corresponding AREMA specification [9].

As the current test program concentrated on the behaviour of the IRJ assemblies under cyclic loading conditions and the characteristics of the joint bar materials, the relevant qualification requirements are discussed in more detail below.

Cyclic load test

For the joint assemblies examined in the current tests, the service conditions may include axle loads of up to 40 tonnes, and ballasted track with sleeper spacing in the range 600-700mm. The relevance of the current test conditions to these service conditions can be examined by means of the equivalent response of the parent rail section, and the fatigue test requirements for qualification of other track components, such as aluminothermic welds, which are subjected to similar cyclic loading conditions in service.

Qualification requirements for aluminothermic welds under the previous (now superseded) Australian Standard (AS1085.15, [13]) included fatigue testing of welds under 3-point loading, with a maximum load equivalent to that required to develop a maximum longitudinal stress of 230MPa at the underside of the rail foot in the parent rail section, and a test duration of 3 million cycles. For 68kg/m rail and a 1m span, the required load is 428kN. The minimum load used is typically 10kN.

The current standard for qualification of aluminothermic welds (AS1085.20, [14), and the equivalent Euronorm standard [15], utilise a four-point loading arrangement with upper and lower spans defined in terms of the width of the weld collar and the height of the rail section. These parameters, and the applied load, may be varied in order to produce the required stress levels in the equivalent the parent rail section, which in AS1085.20 is also 230MPa.

The loading conditions in AS1085.12 can also be compared with the corresponding AREMA requirements. The latter involve a rolling load test which subjects the joint assembly to both uplift and downward forces. The maximum tensile stress occurs when the load is directly over the centre of the joint; in addition a compressive stress is developed when the rolling load is at the extremity of travel.

Table 4 compares the above procedures on the basis of the maximum stress level and total stress range at underside of the foot, and the number of load cycles. Those described in AS1085.12 and AS1085.15 are directly comparable, as both utilise 3-point loading with a fixed load position. In the AREMA test, the applied load is constant, and the stress varies with the longitudinal position of the roller.

Based on the stress data summarised in Table 4, the fatigue test requirements for IRJ assemblies as outlined in AS1085.12 appear more stringent than the corresponding AREMA requirements. However neither set of loading conditions are equivalent to those required to qualify aluminothermic welds for use under the same service conditions, and which were found to reproduce the failure mode that occurs in the Type A design under the in-track service conditions.

Search

Cover
Foreword
Concurrent Session 1: ROLLING STOCK COMPONENTS
Concurrent Session 2: RAIL
Concurrent Session 3: RAIL SAFETY
Concurrent Session 4: RAIL CAPACITY
Concurrent Session 5: WHEEL/RAIL
Concurrent Session 6: CIVIL STRUCTURES
Concurrent Session 7: SAFETY MANAGEMENT & SIGNALLING
Concurrent Session 8:
Concurrent Session 9: ROLLING STOCK MODELLING
Concurrent Session 10: TRACK STRUCTURE
Concurrent Session 11: CIVIL STRUCTURES
Concurrent Session 12: ELECTRICAL O/H
Concurrent Session 13: WHEEL/RAIL
Concurrent Session 14: PROJECT MANAGEMENT
Concurrent Session 15: ENERGY
Concurrent Session 16: INNOVATION
Concurrent Session 17: ROLLING STOCK
Concurrent Session 18: TRACK CONDITION MONITORING
Concurrent Session 19: ELECTRICAL OVERHEAD
Author Index
Close Document

Table 4: Comparison of fatigue test conditions (68kg rail)

Parameter	*AS1085.12 (IRJ)*	*AS1085.15 (AT weld)*	*AREMA Section 3.8 (IRJ)*
Support span (mm)	1100	1000	914
Load range (kN)	10-290	10-428	196*
Maximum stress at underside of foot (MPa)	172	230	97
Stress range at underside of foot (MPa)	166	225	145
Load cycles (million)	3	3	2

** Constant load applied via rolling load*

Comparison of laboratory test and service conditions

A comparison of the fatigue crack details for the Type A design which failed during the higher load fatigue test with the two in-service failures confirmed that in all cases the fatigue crack initiated at the lower, outer corner of the joint bar. However the critical crack size at failure in the laboratory test, at 28mm, was higher than that in the two in-service failures. The difference in critical crack sizes can be attributed to either higher stress levels under in-service loading, a lower dynamic fracture toughness associated with impact loading (as could be expected under the in-service conditions), or a combination of these two factors. As the primary objective on the comparison of the IRJ types is to identify those in which the probability of fatigue crack initiation is minimised, the fatigue crack size at failure is of secondary importance, other than to demonstrate that the fatigue test conditions are capable of reproducing the in-service failure mode.

Measurement of joint bar stress levels under service loading conditions at two different sites identified differences of up to 70-80% in the maximum stress at the lower flange, and approximately 25% in the maximum stress range [7]. The differences between the IRJ response at the two sites was attributed to variations in rail support conditions, which were also assessed using sleeper displacement measurements. Similar measurements at a third site, which was reportedly more prone to IRJ failures, showed much higher sleeper deflections.

Maximum stress levels under loaded ore cars at the initial two sites were approximately 160MPa and 95MPa, respectively, compared to equivalent values of 230MPa and 330MPa, respectively, in the Type A design under the 290kN and 400kN fatigue test conditions. The laboratory test conditions could therefore be considered more severe than those under in-service loading. However, based on the higher sleeper deflections at the third test site [7], joint bar stress levels at this location could be expected to be closer to those obtained under the laboratory test conditions.

The similarities in joint bar stress levels and failure modes in the Type A design, between the in-service and laboratory test conditions, therefore confirms that increasing the maximum load used for the fatigue test to a level equivalent to that required for aluminothermic welds (i.e. 390kN), may be suitable for qualification testing of IRJ assemblies in 68kg rail for the above service conditions.

Joint bar materials

Material requirements for fish plate or joint bars are covered in both Australian (AS) and North American (AREMA) specifications. For the Australian standard, these are presumably those in AS1085.2 for Fishplates [12], although it is noted that AS1085.12 does not explicitly define the requirements for the joint bars or fishplates. The AREMA specification is more explicit in this regard, with Section 2.11 (Specifications for bonded insulation rail joints) referencing Section 2.8 (Specifications for quenched carbon-steel joint bars, microalloyed joint bars, and forged compromise joint bars) for the material requirements.

The two sets of standards allow for either hot-rolled or forged products. The relevant material parameters are the mechanical properties (yield and tensile strength, elongation, reduction of area); these requirements are summarised in Table 5.

Table 5: Material strength requirements for joint bars

Parameter	*AS1085.2*	*AREMA Section 2.8*
Yield strength (MPa)	Not specified	483 (min)
Tensile strength (MPa)	550-740	689 (min)
Elongation (%)	13 (min)	12 (min)
RoA (%)	Not specified	25 (min)

The AREMA specification also includes a limit of 0.040in (1mm) maximum depth of decarburised layer in quenched carbon steel forged bars and forged compromise bars; however no corresponding value is specified for microalloyed

Cover
Foreword
Concurrent Session 1: ROLLING STOCK COMPONENTS
Concurrent Session 2: RAIL
Concurrent Session 3: RAIL SAFETY
Concurrent Session 4: RAIL CAPACITY
Concurrent Session 5: WHEEL/RAIL
Concurrent Session 6: CIVIL STRUCTURES
Concurrent Session 7: SAFETY MANAGEMENT & SIGNALLING
Concurrent Session 8:
Concurrent Session 9: ROLLING STOCK MODELLING
Concurrent Session 10: TRACK STRUCTURE
Concurrent Session 11: CIVIL STRUCTURES
Concurrent Session 12: ELECTRICAL O/H
Concurrent Session 13: WHEEL/RAIL
Concurrent Session 14: PROJECT MANAGEMENT
Concurrent Session 15: ENERGY
Concurrent Session 16: INNOVATION
Concurrent Session 17: ROLLING STOCK
Concurrent Session 18: TRACK CONDITION MONITORING
Concurrent Session 19: ELECTRICAL OVERHEAD
Author Index
Close Document

joint bars produced from hot-rolled sections. No limits on decarburisation are included in AS1085.2.

Examination of the joint bars which failed in service, and the fatigue test results for the Type A design, highlight the importance of the near-surface characteristics in the most highly-stressed locations in the joint bars. On this basis, consideration should be given to introduction of tighter limits, particularly for components intended for use under high axle load conditions.

The tensile strength requirements in AS1085.2 also appear inadequate, based on the maximum stress levels measured in the current tests. Aligning the AS requirements with those in the AREMA specification should be considered.

CONCLUSION

The test program outlined in this paper demonstrated that the reliability of IRJ assemblies under heavy haul conditions could be improved through one or a combination of design changes, including:

- Manufacture of joint bars using a quenched and tempered steel (such as Bisalloy 80) prepared such that there is no measureable near-surface decarburisation.
- Use of a similar material in a higher modulus joint bar design, as demonstrated by the results for the Type D design.

The test program also provides a basis for specifying qualification requirements over and above those in either AS1085.12 or the AREMA Manual for Railway Engineering.

ACKNOWLEDGEMENTS

Three of the authors (PM, CT and MH) acknowledge the support of Rio Tinto Iron Ore for the work described, and permission to publish the paper.

The assistance of Alan Coram, Andrew Mutton and Paul Curcio for the laboratory test program is gratefully acknowledged.

REFERENCES

1. Preliminary results of prototype insulated joint tests at the Facility for Accelerated Service Testing, US Dept of Transportation Federal Railroad Administration, Research Results RR08-11, December 2008.
2. Davis D.D., Akhtar M. (2006), Reduced impact bonded insulated joint designs, Railway Track and Structures, 102 (8), pp17-19.
3. Plaut R.H., Lohse-Busch H., Eckstein A., Lambrecht S., Dillard D.A.(2007), Analysis of tapered, adhesively bonded, insulated rail joints, Proceedings of the Institution of Mechanical Engineers, Part F: Journal of Rail and Rapid Transit, 221 (2), pp195-204.
4. Davis D.D., Akhtar M.N. (2007), Improved insulated rail joints for high tonnage lines with heavy-axle loads, Railway Track and Structures, 103 (8). Pp.24-29.
5. Nicoli E., Dillard D.A., Campbell J., Dillard J., Turner M.A., Davis D.D., Akhtar M. (2007), Characterizing and improving insulated joints performance, Proceedings of the SEM Annual Conference and Exposition on Experimental and Applied Mechanics, pp.121-128.
6. Nicoli E., Dillard D.A., Dillard J.G., Campbell J., Davis D.D., Akhtar M. (2011), Using standard adhesion tests to characterize performance of material system options for insulated rail joints, Proceedings of the Institution of Mechanical Engineers, Part F: Journal of Rail and Rapid Transit, 225 (5), pp509-521.
7. Mayers A., Dhanasekar M (2012), Measurement of in-service insulated rail joint tie plate response, submitted for presentation at Conf. on Railway Engineering (CORE2012), Brisbane, September.
8. AREMA (2002), Manual for Railway Engineering, Section 2.11, Specifications for bonded insulation rail joints, American Railway Engineering and Maintenance-of-Way Association.
9. AREMA (2002), Manual for Railway Engineering, Section 2.8, Specifications for quenched carbon-steel joint bars, microalloyed joint bars, and forged compromise joint bars, American Railway Engineering and Maintenance-of-Way Association.
10. McKelvey S.A., Fatemi A. (2012), Surface finish effect on fatigue behaviour of forged steel, International Journal of Fatigue, 36 (1), pp.130-145.
11. Standards Australia (2002), AS1085.12-2002, Railway track material, Part 12: Insulated joint assemblies.
12. Standards Australia (2002), AS1085.2-2002, Railway track material, Part 2: Fishplates.
13. Standards Australia (1995), AS1085.15-1995, Railway track material, Part 15: Aluminothermic rail welding, (superseded).
14. Standards Australia (2012), AS1085.20-2012, Railway track material, Part 20: Welding of steel rail.
15. CEN (2006), EN14730-1, Railway applications – Track – Aluminothermic welding of rails – Part 1: Approval of welding processes.

Cover
Foreword
Concurrent Session 1:
ROLLING STOCK COMPONENTS
Concurrent Session 2:
RAIL
Concurrent Session 3:
RAIL SAFETY
Concurrent Session 4:
RAIL CAPACITY
Concurrent Session 5:
WHEEL/RAIL
Concurrent Session 6:
CIVIL STRUCTURES
Concurrent Session 7:
SAFETY MANAGEMENT & SIGNALLING
Concurrent Session 8:
Concurrent Session 9:
ROLLING STOCK MODELLING
Concurrent Session 10:
TRACK STRUCTURE
Concurrent Session 11:
CIVIL STRUCTURES
Concurrent Session 12:
ELECTRICAL O/H
Concurrent Session 13:
WHEEL/RAIL
Concurrent Session 14:
PROJECT MANAGEMENT
Concurrent Session 15:
ENERGY
Concurrent Session 16:
INNOVATION
Concurrent Session 17:
ROLLING STOCK
Concurrent Session 18:
TRACK CONDITION MONITORING
Concurrent Session 19:
ELECTRICAL OVERHEAD
Author Index
Close Document

Search